JBUON 2020; 25(1): 531-542
ISSN: 1107-0625, online ISSN: 2241-6293 • www.jbuon.com
Email: editorial_office@jbuon.com

ORIGINAL ARTICLE

Anti-cancer effects of recombinant arazyme from *Serratia Proteomaculans*

Ghazaleh Amjadi[1], Kazem Parivar[1], Seyed Fazlollah Mousavi[2], Abbas Ali Imani Fooladi[3]

[1]Department of Biology, Science and Research Branch, Islamic Azad University, Tehran, Iran; [2]Department of Bacteriology & Microbiology Research Center, Pasteur Institute of Iran, Tehran, Iran; [3]Applied Microbiology Research Center, Systems Biology and Poisonings Institute, Baqiyatallah University of Medical Sciences, Tehran, Iran.

Summary

Purpose: *Colorectal cancer is a lethal and prevalent type of cancer in both men and women worldwide, which can develop resistance to cancer chemotherapy. Developing an effective therapeutic agent is the most promising method for this life-threatening disease. The present study aimed to identify, clone, express and purify the recombinant arazyme (r-arazyme) of Serratia proteomaculans and evaluate the antitumor effect of r-arazyme in vitro.*

Methods: *Bacterial strains and cell line, construction of expression vector and preparation of recombinant protein were prepared and then evaluated by western blot, cell culture, cell viability assay, lactate dehydrogenase release assay, cell apoptosis assay, caspase-3 and -9 activation assay, adhesion assay, matrigel invasion assay and reverse transcriptase-polymerase chain reaction (RT-PCR).*

Results: *R-arazyme caused a great cytotoxic effect against human colorectal adenocarcinoma (HT29) cells in a dose-dependent manner, without any cytotoxic effect on human embryonic kidney cells 293 (HEK 293). In addition, r-arazyme could induce apoptosis in colorectal cancer cell lines via caspase-3 activation and the elevation of the Bax/Bcl-2 ratio. Further, r-arazyme inhibited cancer cells angiogenesis by significantly reducing the expression of angiogenesis-related genes such as VEGF, VEGFR-1, and VEGFR-2. Furthermore, r-arazyme could prevent invasion and adhesion of cancer cells. In general, the results may support the evidence that r-arazyme is a promising therapeutic candidate against cancer.*

Conclusion: *R-arazyme may play an important role in developing effective therapies against colorectal adenocarcinoma in humans, which results in reducing the overall morbidity and mortality related to colorectal cancer.*

Key words: *recombinant arazyme, colorectal cancer, angiogenesis, apoptosis, anti-tumor*

Introduction

Colorectal cancer is the second and third highly lethal and most prevalent malignancy in females and males, respectively, which presents a major challenge to healthcare systems around the world, due to its difficult early diagnosis, dormant course, metastasis, strong invasion, and poor prognosis [1-4]. The International Agency for Research on Cancer reported that about 1.2 million new cases of colorectal cancer were diagnosed worldwide in 2008, accounting for 8% of all cancer-related mortality [5,6]. In 2016, the incidence of new cases of colorectal cancer in the United States and China increased to 134,490 and 274,841 respectively, which accounted for 48% colon-related mortality [5,7]. In the developed countries, economic development and rapid urbanization followed by dietary and lifestyle changes resulted in high morbidity and mortality-related colorectal cancers [8]. In addition, the incidence and mortality of colorectal cancer have increased in developing countries during recent

Corresponding author: Abbas Ali Imani Fooladi, PhD. Applied Microbiology Research Center, Systems Biology and Poisonings Institute, Baqiyatallah University of Medical Sciences, Mollasadra Ave.14359-41711, Tehran, Iran.
Tel/Fax: +982188068924, Email: imanifouladi.A@gmail.com, Imanifouladi.A@bmsu.ac.ir
Received: 31/05/2019; Accepted: 04/07/2019

years, which is higher than that of the world average [9]. Presently, the standard chemotherapeutic regimens based on leucovorin or 5-Fluorouracil (5-FU) for colon cancer patients are frequently attenuated by developing resistance to a wide spectrum of the classic anticancer agents and considerable side effects such as systemic toxicity [10-12]. Further, at the time of diagnosis, 50% out of 80% patients who were subjected to curative surgical resection, will develop of metastatic disease [13]. The high incidence and mortality of colorectal cancer combined with the paucity of effective anticancer agents highlight the urgent need for designing effective therapeutic approaches in order to help develop newer treatments and control the disease among the patients worldwide. Evaluating and identifying plant- and bacterial-derived anticancer agents have paved the way for developing the new therapeutic agents for a few treatment options of metastatic colorectal cancer.

Furthermore, the administration of exogenous proteases such as trypsin and chymotrypsin could effectively prevent tumor growth in different animal models of experimental tumors [14]. Treating mice with fastuosain, which is the purified cysteine protease of *Bromelia fastuosa* has protective effects against tumor development by reducing the number of lung nodules in a murine metastatic melanoma model, which was related to a direct effect on tumor cell migration [15,16]. Recently, the metalloprotease arazyme has shown a strong antitumor effect in a murine metastatic melanoma by inducing cleavage of tumor cell surface CD44 and tumor matrix metalloprotease 8 (MMP-8) antibodies [17,18]. Along with its proteolytic-dependent activity, it has been purported that arazyme can activate macrophages and dendritic cells, and increase surface activation markers and proinflammatory cytokine secretion through TLR4-MyD88-TRIF- and MAPK-dependent signaling pathways [17]. In addition, it can enhance IFNγ-dependent, $CD8^+$ and $CD4^+$ T, as well as B lymphocytes responses involved in inducing antitumor response [17]. Arazyme, a 51.5 kDa metalloprotease of *Serratia proteamaculans*, is a symbiotic bacterium from the *Nephilaclavata* spider encoded by the *araA* gene [19]. The antitumor activities of bacterial-derived proteases have less been emphasized.

The present study aimed to investigate whether recombinant arazyme (r-arazyme) could have cytotoxic activity against HT-29 (human colorectal adenocarcinoma) cell line to induce apoptosis and reduce adhesion/invasion of these cells. To this aim, the cytotoxic potential of r-arazyme was evaluated by considering various aspects involved in r-arazyme anticancer effects *in vitro*.

Methods

Bacterial strains and cell line

Escherichia coli BL21 (DE3) as expression bacterial host was preserved in our laboratory. HT-29 (human colorectal adenocarcinoma) and HEK 293 (Human embryonic kidney cells 293) cell lines were purchased from Pasteur Institute (Tehran, Iran).

Construction of expression vector

The complete arazyme-encoded gene (*araA*) of *S.proteamaculans* (GenBank Accession No: AY818193.1) was inserted into an expression vector pET28a, in the frame with a T7 promoter kanamycin resistant gene and the C-terminal six-His-tagged sequence. *BamHI* and *XhoI* (Fermentas, Lithonia) restriction sites were located at the 5' end and the 3' end of *araA* gene, respectively. Then, the recombinant gene construct pET28a/*araA* was synthesized by Biomatik Corporation (Cambridge, Ont., Canada) and subsequently verified by PCR, restriction digestion, and DNA sequencing. In addition, specific primers were designed for *araA* sequences of *S. marcescens* including forward 5'-CGCTATCGCTCACTGCACTA-3' and reverse 5'-CGGGGCTTTCAAAGTTCAGC-3'. Amplifications were conducted by using *Pfu* DNA polymerase (Fermentas, Lithonia) in 30 cycles, with the cycle parameters including predenaturation at 94°C for 1 min, denaturation at 94°C for 1 min, annealing at 60°C for 1 min, elongation at 72°C for 1 min, and a final extension at 72°C for 5 min. Further, the recombinant construct was cleaved with *BamHI* and *XhoI*.

Preparation of recombinant protein

The recombinant gene construct was overexpressed, and the protein was affinity-purified by a Ni-NTA agarose-based procedure following an on-column re-solubilization protocol, as previously described [20-23]. Briefly, the overexpression of r-arazyme was induced by adding 1 mM isopropyl β-D-1-thiogalactopyranoside (IPTG; Sigma, USA) to *E. coli* BL21 (DE3) carrying the recombinant gene construct culture for 2, 4, 6 and 12 h. Then, the bacterial cells were pelleted and dissolved in a lysis buffer (50 mM NaH2PO4, 300 mMNaCl, and 1 mM PMSF at pH 8.0). Then, the suspension was centrifuged, the supernatant was mixed with Ni-NTA resins (QIAGEN, Germany), and treated with washing buffers with decreasing urea concentrations (8, 6, 4, 2, 1, 0 M urea). Finally, the arazyme was eluted with 250mM imidazole solution. In order to remove imidazole, the protein solution was dialyzed against phosphate buffered saline (PBS) (pH 7.4) overnight. The total amount of purified solubilized protein from 1 L of bacterial culture was quantitatively measured by using a NanoDrop 2000 spectrophotometer system (Thermo Scientific, USA). In addition, the r-arazyme protein was tested for lipopolysaccharide (LPS) contamination by using a commercially available Pierce™ LAL Chromogenic Endotoxin Quantitation Kit.

Western blot

The r-arazyme was electrophoresed by SDS-PAGE with 12.5% polyacrylamide mini-gels and then trans-

ferred onto polyvinylidene fluoride (PVDF) membranes (Hi-bond Amersham Biosciences, USA) by using a semi-dry blotting apparatus at 15 volts/10 min (Labconco, Kansas City, MO, USA). The protein was electrotransferred to PVDF membranes (Invitrogen) in a semi-dry transfer cell at 15 volts/10 min (Trans-Blot®SD, Bio-Rad, USA) and washed with Tris-buffered saline with Tween 20 (TBS-T) containing 20 mMTris–HCl (pH 7.4), 0.5 M NaCl, and 0.05% Tween 20 (Merck, Germany). Membrane blots were blocked for one hour with PBS with 1% (w/v) skim milk, and accordingly incubated with mouse anti-His tag monoclonal antibody, with 1:10,000 diluted HRP-conjugated goat anti-mouse antibodies (Sigma, USA). After washing byTBS-T several times, the membranes were developed using a 3, 3'-Diaminobenzidine substrate (DAB). In addition, membrane blots were de-stained with 50% methanol plus 7% acetic acid (5-10min RT). Finally, the images of DAB-stained blots were captured by a digital camera.

Cell culture

HT-29 (human colorectal adenocarcinoma) and HEK 293 (Human embryonic kidney cells 293) cell lines were purchased from Pasteur Institute (Tehran, Iran). Then, the cells were cultured as a monolayer in RPMI-1640 medium (Gibco, Germany) including10% fetal bovine serum (FBS, Gibco) and 1% penicillin/streptomycin (100 U/mL penicillin and 100 mg/L streptomycin 100 µg/mL; Gibco) at 37°C in the presence of 5% CO_2.

Cell viability assay

Cell viability assay was evaluated with 3-(4, 5-dimethylthiazol-2-yl)-2,5-diphenyltetrazolium bromide (MTT) as it was already described [24,25]. Briefly, 1×10^5 cells/mL were cultured in 96-well plates (Nunc; Naperville, IL) and treated with 5, 10, 16, 32, 64, 128 and 256 µg/ml of r-arazyme for 24 h. Then, the cells were subsequently treated with MTT solution (Sigma-Aldrich; Merck Millipore) at 37°C in a 5% CO_2 incubator for 4 h. In the next procedure, the culture medium was replaced by 200 µl DMSO and the absorbance was measured at 570nm by using an ELISA microplate reader [26]. The percentage of cytotoxicity activity was calculated as follows: Cytotoxicity activity (%) =[1−(absorbance of experimental well/ absorbance of negative control well)] ×100.

Lactate dehydrogenase (LDH) release assay

Lactate dehydrogenase (LDH) release assay was performed as previously described [27]. Briefly, HT-29 cells were incubated with different concentrations of r-arazyme for 24 h. Then, the cells were lysed with 2% (v/v in PBS) Triton X-100 (Sigma, USA) and mixed with 100 µl of the LDH reaction solution for 30 min. Finally, the absorbance of the reaction mixture was measured at 490 nm by using an ELISA microplate reader.

Cell apoptosis assay

Annexin V-FITC/PI staining assay was performed to identify apoptotic cells as previously described [28]. Briefly, HT-29 cells (2×10^5 cells/well) were treated with different concentrations of r-arazyme on 6-well tissue culture plates for 24 h. The cells were subsequently trypsinized and centrifuged at 1500×g for 5 min to remove the cell culture supernatant. Then, the cells were stained with annexin V-FITC (5 mg/ml) solution (BD, San Diego, CA, USA) and PI (6 mg/ml) (Sigma) for 20 min in the dark. Finally, the cells were analyzed by using a FACScan flow cytometer [27] and FLOWJO software version 9.0 (Tree Star, USA).

Caspase-3 and -9 activation assay

Caspase-3 and -9 activities were measured by using a caspase-3 or -9 colorimetric assay kit (Abcam, Cambridge, MA, USA) according to the manufacturer's instructions. First, r-arazyme treated and untreated cells were dissolved in a lysis buffer of HEPES, pH 7.4, 0.1% CHAPS, 1 mmol/L DTT, 0.1 mmol/L EDTA and 0.1% Triton X-100 and incubated for 30 min on ice. Then, the suspension was centrifuged and the supernatant was mixed with reaction buffer containing 2 mmol/L Ac-DEVD-AFC for caspase-3 and LEHD-AFC for caspase-9 in a caspase assay buffer at 37°C with 10 mmol/L DTT for 30 min. Finally, caspase activity was determined by measuring the absorbance at 405 nm.

Adhesion assay

Adhesion assay was performed as previously described [17]. First, r-arazyme-treated and untreated cells were washed twice with PBS and fixed with methanol. Then, the cells were subsequently stained with toluidine blue 1% in sodium tetraborate 1% and solubilized in SDS 1%. Finally, the absorbance at 540 nm was measured after developing the color.

Matrigel invasion assay

As it was already mentioned, the matrigel invasion assay was performed [17]. First, the upper and lower transwell chambers (8-mm pore size, Corning Costar Co., MA, USA) were filled with RPMI-diluted Matrigel (Basement Membrane Matrix, BD Biosciences, NJ, USA) and RPMI (Gibco, Germany) containing 10% FBS, respectively. Then, r-arazyme-treated and untreated cells were added to the upper chambers and incubated for 5h at 37°C in 5% CO_2. After removing non-invading cells, the cells underneath the membrane filter were fixed in paraformaldehyde and stained with toluidine blue solution. Finally, the suspension was solubilized in SDS 1% and the absorbance was measured at 600 nm.

Reverse transcriptase-polymerase chain reaction

The mRNA expression of apoptosis regulatory genes (Bax and Bcl-2) and angiogenesis genes (VEGF-A, VEGFR-1, and VEGFR-2) were measured by SYBR Green real-time PCR analysis by using specific oligonucleotide primers [29-31]. Then, the total RNA of treated and untreated cells was extracted by using a TRIZOL reagent (Invitrogen, USA), which was used for cDNA synthesis by implementing a RevertAidTMfirst stranded cDNA Synthesis Kit (Fermentas, Lithonia). Glyceraldehyde 3-phosphate dehydrogenase (GAPDH) gene was utilized as an endogenous control. The PCR reaction mixture included 12.5 µl of SYBR Green Master Mix,

400 ng of template DNA, forward and reverse primers (0.25 µM each), and 12 µl of nuclease-free water. Finally, RT-PCR was cycled between 95°C for 15 s and 60°C for 1 min for 40 cycles, after a 95°C denaturation step for 5 min.

Statistics

Statistical analyses were performed by IBM SPSS Statistics for Windows, Version 21.0 (IBM Corp. Released 2012. Armonk, NY: IBM Corp.) and GraphPad Prism 6 (GraphPad Prism version 6.00 for Windows, GraphPad Software, La Jolla California USA). Normally distributed data were analyzed by ANOVA with Tukey's multiple comparison tests. Nonparametric data were analyzed by Kruskal-Wallis U test followed by multiple comparison tests. The results were expressed as the mean ± standard error of the mean [32], and p value <0.05 was considered as statistically significant.

Results

Cloning and expression of the r-arazyme

Agarose gel electrophoresis of the PCR product indicated a single band with the expected sizes of 1,482b prepresenting the amplification of the *araA* gene (Figure 1A). In addition, the presence of the *araA* gene recombinant construct (pET-28a/*araA*) was verified by *BamHI* and *XhoI* digestion (Fig. 2B). Finally, the identity and orientation of the *araA* gene recombinant construct were confirmed by DNA sequencing (data not shown).

In the next procedure, the protein expression of *E. coli* BL21 (DE3) carrying recombinant vector was induced with IPTG (1 mM). Based on SDS-PAGE gel, the expression product of r-arazyme protein was approximately 51.5kDa. The r-arazyme was successfully purified by Ni–NTA affinity chromatography under denaturing procedures and 65 mg of highly purified r-arazyme was obtained from one liter of the induced culture (Figure 3C). As illustrated in Figure 4D, based on western blot analysis, anti-His monoclonal antibody reacted specifically with a ~51.5kDa, protein in *E. coli* BL21 (DE3) lysates, corresponding to r-arazyme.

R-arazyme has high cytotoxic activity against HT-29 cell

First, the cytotoxic activity of r-arazyme against HT-29 cells was determined by MTT assay.

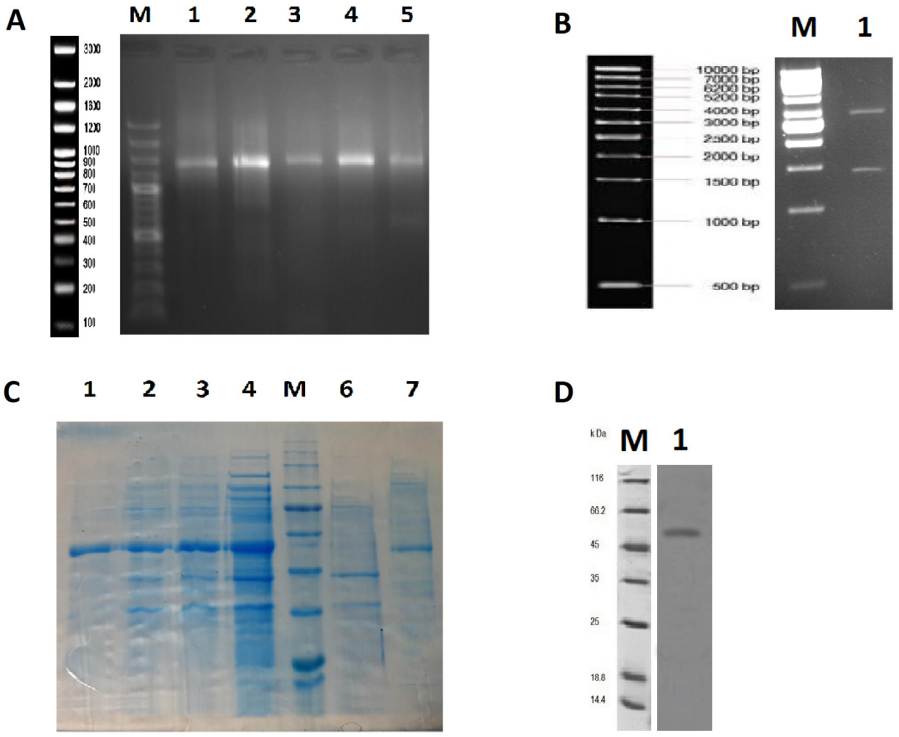

Figure 1. Screening *araA* gene and protein by restriction enzyme digestion and Immunobloting methods. Analysis of the PCR product following the amplification of the *araA* gene; Lane M, DNA size marker; lane 1-5, PCR product resulting from the amplification of the *araA* gene **(A)**. Screening *araA* gene by restriction enzyme digestion. The plasmids were extracted and digested with the appropriate restriction enzymes. Lane 1, pET22b-*araA* digested with *BamHI* and Xho1; lane M, DNA size marker **(B)**. SDS PAGE for detecting expressed and purified r-arazyme; Lane M, low molecular weight protein size markers; lane 1, 2, 3 and 4, ~51 kDa induced arazyme protein from bacterial cultures after 2, 4, 6 and 12 h of induction; lane 6, pellet of un-induced bacteria; lane 7, purified r-arazyme **(C)**. Immunobloting results; Lane 1, crude cell lysate of 4 h-induced bacteria detected by monoclonal anti-His tag antibody; Lane M, low molecular weight protein size markers **(D)**.

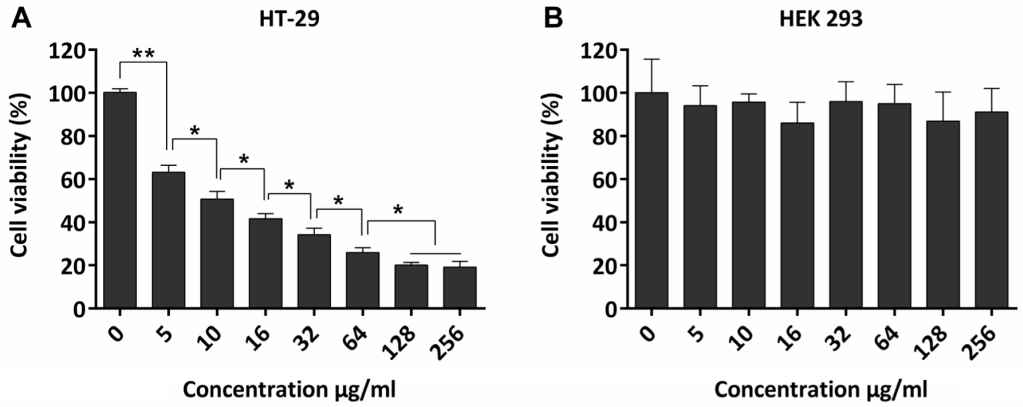

Figure 2. The comparative analysis of cytotoxic effects of r-arazyme on HT29 and HEK 293 cell lines. HT29 **(A)** and HEK 293 **(B)** cell lines were incubated with different amounts of r-arazyme (5-256 µg/ml). HEK 293 cell line was used as a control. Data represent the mean±SEM of three independent experiments. *p<0.05 and **p<0.01 indicate the groups which were significantly different.

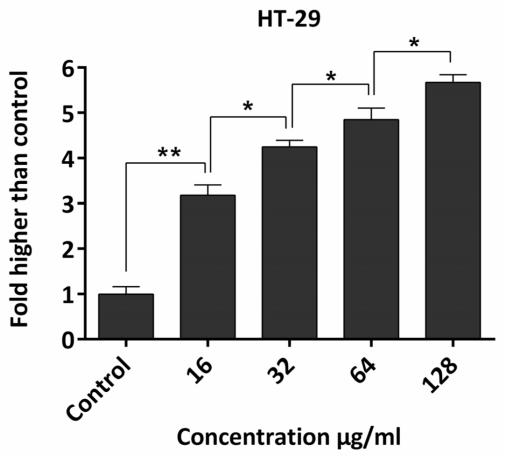

Figure 3. The comparison of LDH released from the r-arazyme treated and untreated- HT29 cells. The level of released LDH from HT-29 cells after 24 h of treatment with different amounts of r-arazyme (16-128 µg/ml) was measured by LDH leakage assay. Data represent the mean±SEM of three independent experiments. *p<0.05 and **p<0.01 indicate the groups which were significantly different.

HEK 293 cells were used as control. As shown in Figure 2A, r-arazyme significantly decreased HT29 cell viability in a dose-dependent manner. R-arazyme at 128 and 256 µg/ml concentrations showed the highest cytotoxic activity against HT-29 cells, with the cell viability of 29 and 19%, respectively ($p<0.05$). As displayed in Figure 2A, the cytotoxic activity of r-arazyme against HT-29 cells at all concentrations was significantly higher than that of untreated cells ($p<0.01$), which was 21.01 µg/ml for the IC_{50} value of r-arazyme. It is worth noting that r-arazyme at all concentrations was found to have no cytotoxic activity on HEK 293 cells (Figure 2B). Further, no significant difference was found regarding the cytotoxic activity of r-arazyme between 24 and 48 h treatments.

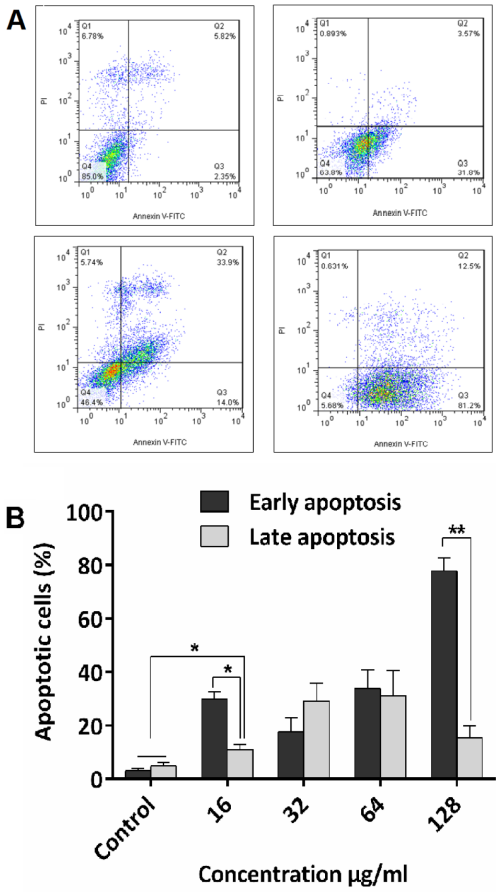

Figure 4. The effect of r-arazyme on HT-29 cell apoptosis. HT-29 cells were treated with 16-128 µg/ml of r-arazyme and then, annexin V/PI staining using flow cytometry was performed. **(A):** Flow cytometry analysis of HT-29 cells was treated with 16, 32, 64, and 128 µg/ml r-arazyme for 24 h. **(A):** Representative scatter plots of PI (y-axis) vs. annexin V (x-axis). Representative figures showing the population of viable (annexin V- PI-), early apoptotic (annexin V+ PI-), late apoptotic (annexin V+ PI+) and necrotic (annexin V- PI+) cells. **(B):** The percentage of early and late apoptotic cells. Data represent the mean±SEM of two independent experiments. *p<0.05 and **p<0.01 indicate the groups which were significantly different.

Furthermore, the LDH enzyme leakage assay was performed to confirm the cytotoxic effects of r-arazyme against HT-29 observed in MTT assay. Following r-arazyme treatment, LDH leakage increased significantly and dose-dependently in HT-29 cells, compared to the untreated cells ($p<0.05$; Figure 3). As shown in Figure 6, r-arazyme at concentrations 16, 32, 64, and 128 μg/ml caused the increase of 3.1-, 4.2-, 4.8-, and 5.6-fold ($p<0.01$) in the LDH release than the untreated control, confirming the observed cytotoxicity in MTT assay. However, this cytotoxic effect was not observed in HEK 293 cells.

R-arazyme induces apoptosis of HT-29 cells

Annexin V and PI staining were conducted to see whether the cytotoxic effect of r-arazyme on HT-29 is related to apoptosis or not. As shown in Figure 4A, r-arazyme-treated cells indicated a significant decrease in the percentage of viable cells in a dose-dependent manner. R-arazyme significantly increased the percentage of early apoptotic cells from 3% in untreated cells at the concentrations of 16, 32, 64, and 128μg/ml to 29.9, 17.65, 33.7, and 77.8%, respectively ($p>0.05$ [OR $P<0.05$?]; Figures 4A-B). In addition, the population of late-stage apo-

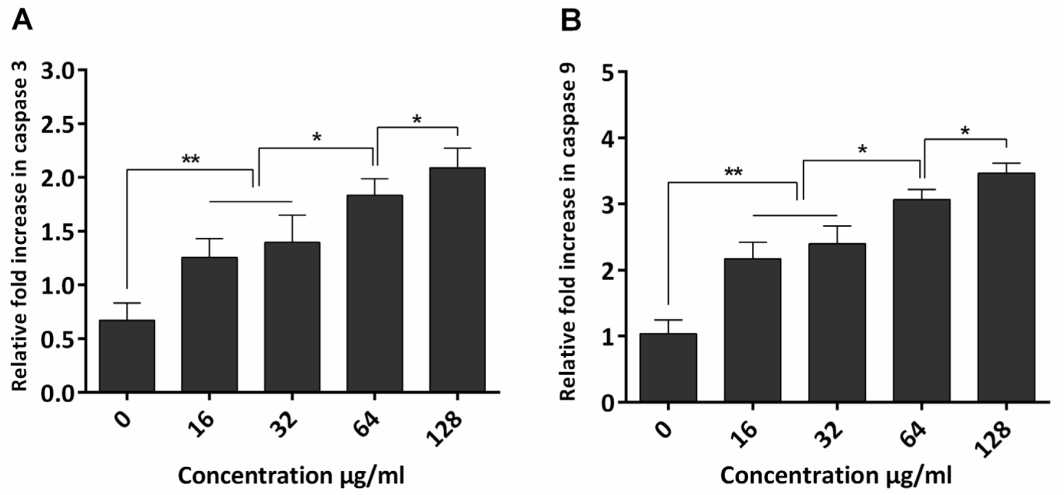

Figure 5. A comparative analysis of r-arazyme effects on caspase-3 and –9 activations in HT-29 cells. The relative fold caspase-3 **(A)** and -9 **(B)** activity were measured in HT29 treated cells with 16-128 μg/ml of r-arazyme. Data represent the mean±SEM of three independent experiments. *$p<0.05$ and **$p<0.01$ indicate the groups which were significantly different.

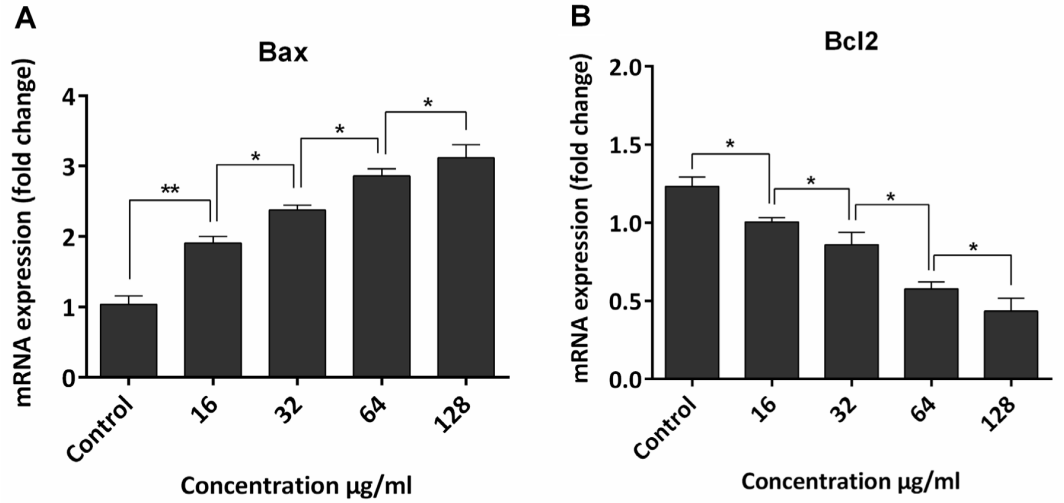

Figure 6. Quantitative PCR analysis of apoptosis-associated genes in r-arazyme-treated HT-29 cells. HT-29 cells were treated with 16-128 μg/ml of r-arazyme. The total RNA was isolated and converted to single-stranded cDNAs, which were then quantified by real-time PCR using sybr green and primer pairs pre-designed for Bax **(A)**, Bcl-2 **(B)** and GAPDH as an endogenous control. Relative mRNA levels of Bax and Bcl-2 in treated HT29 cells versus untreated cells are expressed as the mean ± SD of at least three independent experiments. *$p<0.05$ and **$p<0.01$ indicate the groups which were significantly different.

ptotic cells after treatment with 16, 32, 64, and 128 µg/ml of r-arazyme significantly increased to 10.95, 29.11, 31 and 15.5 %, respectively, compared to the amounts in the untreated-cells (4.78%) ($p<0.05$; Figure 4A-B). Further, as illustrated in Figures 4A-B, the number of early cells increased significantly in the presence of 16 and 128 µg/ml of the r-arazyme ($p<0.05$), compared to the amounts in the late apoptotic cells ($p>0.01$).

In addition, the caspase 3 and 9 activities in HT-29 cells were measured to evaluate the cell apoptosis pathway induced by r-arazyme. As illustrated in Figures 5A-B, r-arazyme increased caspase 3 and 9 activities in a dose-dependent manner. Further, r-arazyme significantly increased the caspase 3 activity at the concentrations of 16, 32, 64, and 128 µg/ml by the folds of 1.8, 1.9, 3, and 3.1, respectively, compared to the amounts in the untreated cells ($p<0.01$; Figure 5A). Further, caspase 9 activity after treatment with 16, 32, 64, and 128 µg/ml of r-arazyme significantly increased by 2, 2.4, 3, and 3.4 fold, respectively, compared to the amounts in the untreated cells ($p<0.01$; Figure 5B).

In the next procedure, the expression level of apoptosis-related genes, Bcl-2, and Bax were assessed in r-arazyme treated HT29 cells by RT-PCR. Then, the relative expression of the gene was determined by dividing its expression amount to that of the GAPDH gene. As shown in Figures 6A-B, the incubation of cells with increasing concentrations of r-arazyme resulted in decreasing the expression of anti-apoptotic Bcl-2 mRNA significantly, associated with a marked increase in the expression of pro-apoptotic Bax mRNA in a dose-dependent manner ($p<0.05$). As illustrated in Figure 6A, the expression level of Bax mRNA increased 1.9, 2.3, 2.8 and 3.1 folds after treatment with 16, 32, 64, and 128 µg/ml of r-arazyme, respectively. Furthermore, the expression level of Bcl-2 gene decreased 0.1, 0.8, 0.5 and 0.4 folds when the HT29 cells were treated with 16, 32, 64, and 128 µg/ml of r-arazyme (Figure 6B).

The role of r-arazyme in decreasing tumor cell adhesion, invasion and metastasis

In order to assess the anti-adhesive effects of r-arazyme, HT29 cells were incubated with different concentrations of r-arazyme, and attached cells were colorimetrically quantitated by using an ELISA reader. As shown in Figure 7, r-arazyme could significantly decrease cell adhesion in a concentration-dependent manner ($p<0.05$). The treatment of tumor cells with 128 µg/ml of r-arazyme indicated the highest anti-adhesive effects, with a 52% reduction in cell adhesion ($p<0.05$; Figure 7). In addition, the adhesions of HT29 cells treated with 64 µg of r-arazyme was significantly reduced by 44%, compared to the amounts at 32 and 16 µg concentrations ($p<0.05$, Figure 7). Further, 72% reduction in cell adhesion was observed under 32 µg/ml of r-arazyme treatment, which was significantly higher than 16 µg/ml treatment group ($p<0.05$). Finally, the treatment of tumor cells with 16 µg/ml of r-arazyme significantly reduced cell adhesion, compared to the untreated cells ($p<0.05$).

In the next procedure, Matrigel invasion assay was performed to determine the inhibitory effects of r-arazyme on colon cancer cell invasion. As displayed in Figure 8, r-arazyme decreased HT29 cells cell invasion to the matrigel-coated substrate in a

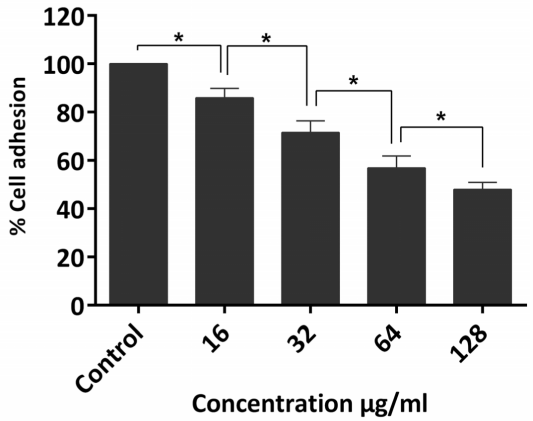

Figure 7. The effect of r-arazyme on HT-29 cell adhesion. HT-29cells were treated with 16, 32, 64, and 128 µg/ml r-arazyme for 24 h, plated on 96-wells plate, and non-adherent cells were removed by a PBS rinse and adherent cells were stained after incubation for 3 hours. Data represent the mean±SEM of three independent experiments. *$p<0.05$ indicates the groups which were significantly different.

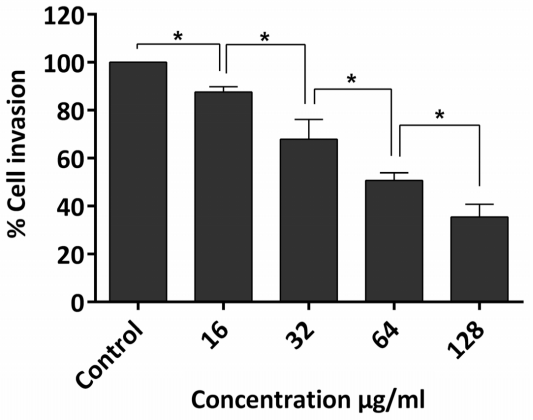

Figure 8. The effect of r-arazyme on HT-29 cell invasion. The ability of HT-29cells-treated with different amounts of r-arazyme (16-128 µg/ml) to invade matrigel was evaluated as described in materials and methods. Data represent the mean±SEM of three independent experiments. *$p<0.05$ indicates the groups which were significantly different.

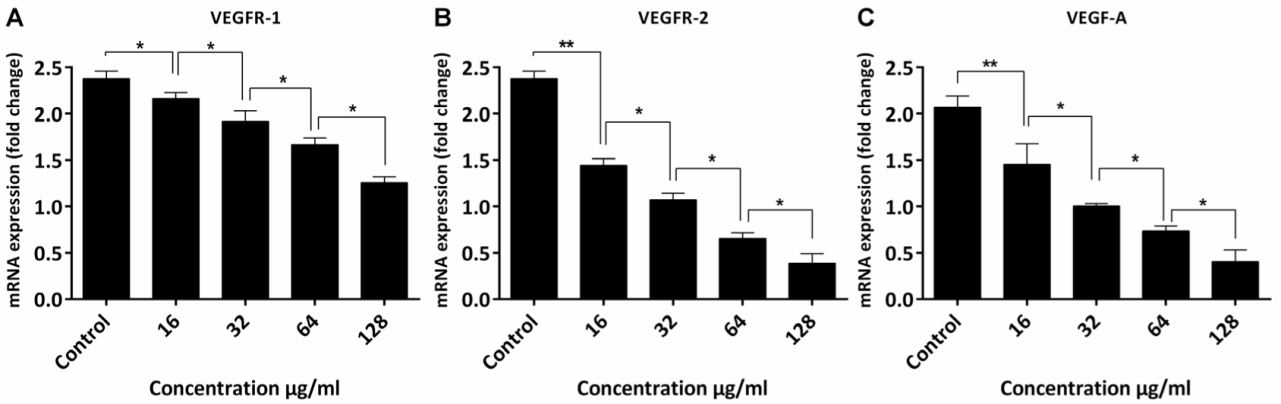

Figure 9. Quantitative PCR analysis of angiogenesis-associated genes in r-arazyme-treated HT-29 cells. HT-29cells were treated with 16-128 µg/ml of r-arazyme. The total RNA was isolated and converted to single-stranded cDNAs, which were then quantified by real-time PCR by using sybr green and primer pairs pre-designed for VEGF-1 **(A)**, VEGFR-2 **(B)**, VEGFR-A **(C)** and GAPDH as an endogenous control. Relative mRNA levels of for VEGF-1, VEGFR-2 and VEGFR-A in treated HT29 cells versus untreated cells are expressed as the mean ± SD of at least three independent experiments. *p<0.05 and **p<0.01 indicate the groups which were significantly different.

dose-dependent manner. In addition, the treatment of HT29 cells with 16, 32, 64, and 128 µg/ml of r-arazyme decreased tumor cells invasion by 65, 50, 67 and 87%, respectively. Finally, significant differences were observed between the different concentration of r-arazyme (p<0.05; Figure 8).

The role of r-arazyme in inhibiting angiogenesis of tumor cells

In order to evaluate the possible anti-angiogenic effect of r-arazyme, VEGF-A, VEGFR-1, and VEGFR-2 mRNA expression were first evaluated by using RT-PCR. Then, the relative expression of the genes was determined by dividing its expression amount to that of the GAPDH gene. The results of data analysis for RT-PCR demonstrated the expression of VEGF-A, VEGFR-1 and VEGFR-2 mRNA in decreasing r-arazyme-treated cell in a dose-dependent manner. As illustrated in Figure 9A, the treatment of HT-29 cells with 16, 32, 64, and 128 µg/ml of r-arazyme significantly reduced the transcription of VEGFR-1 by 2.1, 1.9, 1.6 and 1.2 folds, respectively, compared to the amounts in untreated cells (p<0.05). Further, as shown in Figure 9B, the expression level of VEGFR-2 gene decreased 1.3, 1, 0.6 and 0.4 folds when the HT29 cells were treated with 16, 32, 64, and 128 µg/ml of r-arazyme, respectively. Furthermore, the treatment of HT-29 cells with 16, 32, 64, and 128 µg/ml of r-arazyme decreased the mRNA levels of VEGF-A to 1.4, 1, 0.7 and 0.4 folds, compared to the amounts in untreated cells (p<0.05; Figure 9C). Finally, significant differences were reported between the different concentration of r-arazyme (p<0.05; Figure 9A-C).

Discussion

In this study, the r-arazyme was successfully expressed and characterized. PCR and sequencing analysis revealed that the specifically designed primers in this study amplified an approximately 1,482 bp length fragment, which is consistent with the arazyme gene. When the recombinant vector was induced, SDS-polyacrylamide gels showed an apparent molecular mass of 51kDa [17,19]. In addition, the expression of r-arazyme in a heterogeneous host is related to the misfolding and aggregation of inclusion bodies. In the on-column re-solubilization method, urea-solubilized inclusion bodies are physically immobilized to Ni–NTA resin, and accordingly the denaturing agent is gradually replaced by a non-denaturing buffer [22,33]. This protocol greatly helps the internal localization of hydrophobic domains and efficient superficial positioning of hydrophilic parts in the configured protein [33,34]. In addition, the results of this study indicated that the use of refolding the inclusion body protein on Ni-NTA column resulted in enhancing the yield of soluble proteins.

The results of evaluating the *in vitro* cytotoxic activity of r-arazyme-induced cell death against HT29 cells showed that r-arazyme had anti-proliferative activity in dose-dependent and tumor-selective manner, as reflected by the low IC_{50} values and the absence of cytotoxic effects on HEK 293 cells. In MTT assay, the number of metabolically active viable cells is associated with the intensity of formazan dye produced by mitochondrial dehydrogenase enzyme via the reduction of yellow tetrazolium MTT [35]. Further, LDH as a stable

cytoplasmic enzyme is released from apoptotic and necrotic cell death following irreversible cell membrane damage [36]. The results of LDH assay indicated that r-arazyme in a dose-depended manner led to robust cytotoxic effects toward HT-29, as elucidated by elevating the LDH level and cell permeability, which results in increased cell death. Further, the results of MTT and LDH assays together indicated that r-arazyme plays a great role to inhibit cell proliferation and induce cell death of human colon cancer. Additionally, the results demonstrated that the r-arazyme failed to influence the growth and metabolism of normal cells, which are the most suitable attributes of a therapeutic drug and this potential should be considered for more newer drug development.

In the next procedure, Annexin/PI flow cytometric assay was utilized to evaluate the pathways of cell death induced by r-arazyme. Based on the analysis of flow cytometry, r-arazyme treatment resulted in increasing the numbers of cells undergoing early and late apoptosis. The results suggested that r-arazyme induces translocation of phosphatidylserine from the inner to the outer leaflet of the cell membrane, which is generally accepted as one of the biomarkers of apoptosis [37]. Unlike necrosis, apoptosis is able to preserve tissue homeostasis by removing dead cells by immune cells, such as macrophages, without inducing inflammatory responses, which causes the destruction of normal cells and tissue damage [38]. In addition, to maintain their uncontrolled proliferation, cancer cells show different resistance mechanisms to apoptosis. Thus, the potential of apoptosis-inducing related to r-arazyme can be considered as a possible therapeutic agent against cancer in future studies [39].

Apoptosis or programmed cell death is considered as a highly complex process which can mobilize a number of specific molecules and is classified into caspase-dependent or -independent mechanisms [40]. Further, the caspase-dependent pathway is divided into the extrinsic (death receptor) and the intrinsic (mitochondrial) cascade, as determined by the involvement of caspase-8 or caspase-9, respectively [38]. Additionally, both intrinsic and extrinsic pathways resulted in inactivation of caspase-3 which is involved in the final execution of dying cells while caspase-9 is an initiator caspase involved in the intrinsic pathway [38]. A few studies reported the anticancer effects of r-arazyme but the mechanisms of cancer cell apoptosis have not been clearly elucidated [17,41]. In assessing the molecular mechanism underlying apoptosis process, the results of the present study indicated that r-arazyme could induce a concentration-dependent increase in caspase-9 and -3 activities, which confirm the contribution of intrinsic caspase pathways in the cell death induced by r-arazyme. Further, the apoptotic effects of r-arazyme in HT-29 cells were confirmed by a dose-dependent up-regulation of Bax and down-regulation of Bcl2, which are the key genes in the intrinsic pathway of apoptosis [42]. *In vitro*, anti-tumor proliferation and the activity of many drug components are accomplished through the Bax/Bcl-2 pathways [43-45]. However, *in vivo* the association is created between clinical prognostic factors, Bcl-2 and Bax mRNA expression [46,47]. Interestingly, the protein expression of anti-apoptotic Bcl-2 and pro-apoptotic Bax have been associated with longer survival in NSCLC patients [43]. The down-regulation of Bcl-2 and up-regulation of Bax demonstrated the dysregulation of the associated molecules Bcl-2 and Bax and the activation of caspases-3 and -9 [48,49]. The dysregulation of the mitochondria integrity-associated molecules Bcl-2 and Bax suggested that the activation of the mitochondrial pathway is the main event during apoptosis. These findings support the notion that r-arazyme can reduce the survival dosage-dependently and inhibit the growth of colon cancer cell via both intrinsic and extrinsic apoptosis pathways, which may have a therapeutic potential in managing colon cancer.

It is evident that the development of tumor cell invasion and metastasis are a dynamic multistep process including cell adhesion, proteolytic degradation, migration and angiogenesis [50]. Targeted anti-cancer drugs block cell cycle progression by interfering with specific molecules, which play a critical role in tumor cell growth, survival, migration, and invasion spread of cancer [51,52]. Currently, there is increasing attention to the combination of multiple anticancer agents, which target and interfere with several pathways [53]. Data from the potency assessment of r-arazyme indicated that the effective inhibition of adhesion and invasion of the treated-HT-29 cell is evident by reducing the invaded cell to the matrigel-coated substrate in a dose-dependent manner significantly.

In evaluating the mechanism by which r-arazyme inhibits tumor growth and invasion, we found that r-arazyme could efficiently inhibit the angiogenesis of colon cancer cells, which was confirmed by reducing the expression of angiogenesis-related genes significantly, including VEGF and its tyrosine kinase receptors, VEGFR-1 and VEGFR-2. In addition, the inhibition of angiogenesis is a critical step for cancer prevention and treatment, since exceeding the concentrations of

angiogenesis inhibitors than those of stimulators could potentially inhibit the tumor growth and dissemination to other organs [54]. VEGF, VEGFR-1 and VEGFR-2 are identified as common anti-angiogenic target molecules because they are the key mediators of angiogenesis in both physiological and pathological conditions [55]. VEGF induces a cascade of signaling pathways through binding to VEGFR-1 and VEGFR-2 leading to proliferation, migration, survival, and vascular permeability [56,57]. Although VEGF-A, as a critical factor in angiogenesis induction, has been emerged as an attractive target for anti-angiogenesis treatment, the chronic therapeutic use of anti-VEGF agents is limited due to its side effects. It is worth noting that RT-PCR analysis revealed that r-arazyme can decrease the expression of the VEGF-A, VEGFR-1 and VEGFR-2 transcript gene expression, which can contribute to its anti-tumor activities through inhibiting tumor angiogenesis. Consistent with these observations, endothelial cell invasion assay indicated that the angiogenesis potential of conditioned medium from tumor cells significantly reduced when the related cells were treated with r-arazyme, supporting that r-arazyme is an anti-angiogenesis inhibitor by suppressing VEGF expression in tumor cells.

Conclusions

In conclusion, a novel r-arazyme can be qualified as a therapeutic option against colon cancer because it can elicit robust cytotoxic effect in HT-29 cells by modulating the activity and/or expressing the proteins by regulating the process of cellular apoptosis, adhesion invasion, and angiogenesis. In light of these findings, a thorough assessment of r-arazyme under controlled clinical settings seem warranted against different tumor cells. The results in the present study reinforced the promise that the clinical applications of therapeutic potential for r-arazyme may provide patients with an extended range of protection in the near future, and contribute to the reduction of the high morbidity and mortality related to cancer world over.

Acknowledgements

We hereby wish to thank Islamic Azad University, Science and Research Branch for providing generous financial support.

Conflict of interests

The authors declare no conflict of interests.

References

1. Isik A, Peker K, Firat D et al. Importance of metastatic lymph node ratio in non-metastatic, lymph node-invaded colon cancer: a clinical trial. Med Sci Monit 2014;20:1369-75.
2. Sakurai J, Matsui Y, Hiraki T et al. Single Center Prospective Phase II Trial of CT-guided Radiofrequency Ablation for Pulmonary Metastases from Colorectal Cancer (SCIRO-1401). Acta Med Okayama 2016;70:317-21.
3. Wu W, Guo F, Ye J et al. Pre- and post-diagnosis physical activity is associated with survival benefits of colorectal cancer patients: a systematic review and meta-analysis. Oncotarget 2016;7:52095-103.
4. Markovic S, Dimitrijevic I, Zogovic B, Markovic V, Barisic G, Krivokapic Z. Current trends in clinical genetics of colorectal cancer. JBUON 2016;21:1042-9.
5. Siegel RL, Miller KD, Jemal A. Cancer statistics, 2016. CA Cancer J Clin 2016;66:7-30.
6. Lu ZJ, Lu LG, Tao KZ et al. MicroRNA-185 suppresses growth and invasion of colon cancer cells through inhibition of the hypoxiainducible factor-2alpha pathway in vitro and in vivo. Mol Med Rep 2014;10:2401-8.
7. Chen W, Zheng R, Zhang S et al. Annual report on status of cancer in China, 2010. Chin J Cancer Res 2014;26:48-58.
8. Chen AD, Li H, Li YC, Zeng H. Naphthazarin suppresses cell proliferation and induces apoptosis in human colorectal cancer cells via the B-cell lymphoma 2/B-cell associated X protein signaling pathway. Oncol Lett 2016;12:5211-6.
9. Jin Z, Yan W, Jin H, Ge C, Xu Y. Differential effect of psoralidin in enhancing apoptosis of colon cancer cells via nuclear factor-kappaB and B-cell lymphoma-2/B-cell lymphoma-2-associated X protein signaling pathways. Oncol Lett 2016;11:267-72.
10. Hammond WA, Swaika A, Mody K. Pharmacologic resistance in colorectal cancer: a review. Ther Adv Med Oncol 2016;8:57-84.
11. Taherian A, Fazilati M, Moghadam AT, Tebyanian H. Optimization of purification procedure for horse F(ab´)2 antivenom against Androctonus crassicauda (Scorpion) venom. Trop J Pharm Res. 2018;17:409-14.
12. Cai Z, Yang J, Shu X, Xiong X. Chemotherapy-associated hepatotoxicity in colorectal cancer. JBUON 2014;19:350-6.
13. Kahi CJ, Boland CR, Dominitz JA et al. Colonoscopy Surveillance After Colorectal Cancer Resection: Recommendations of the US Multi-Society Task Force on Colorectal Cancer. Gastroenterology 2016;150:758-68 e11.

14. Wald M. Exogenous proteases confer a significant chemopreventive effect in experimental tumor models. Integr Cancer Ther 2008;7:295-310.
15. Guimaraes-Ferreira CA, Rodrigues EG, Mortara RA et al. Antitumor effects in vitro and in vivo and mechanisms of protection against melanoma B16F10-Nex2 cells by fastuosain, a cysteine proteinase from Bromelia fastuosa. Neoplasia 2007;9:723-33.
16. Khomarlou N, Aberoomand-Azar P, Lashgari AP et al. Essential oil composition and in vitro antibacterial activity of Chenopodium album subsp. striatum. Acta Biologica Hungarica 2018;69:144-55.
17. Pereira FV, Ferreira-Guimaraes CA, Paschoalin T et al. A natural bacterial-derived product, the metalloprotease arazyme, inhibits metastatic murine melanoma by inducing MMP-8 cross-reactive antibodies. PLoS One 2014;9:e96141.
18. Heidari MF, Arab SS, Noroozi-Aghideh A, Tebyanian H, Latifi AM. Evaluation of the substitutions in 212, 342 and 215 amino acid positions in binding site of organophosphorus acid anhydrolase using the molecular docking and laboratory analysis. Bratislavske lekarske listy 2019;120:139-43.
19. Kwak J, Lee K, Shin DH et al. Biochemical and genetic characterization of arazyme, an extracellular metalloprotease produced from Serratia proteamaculans HY-3. J Microbiol Biotechnol 2007;17:761-8.
20. 20. Korpi F, Irajian G, Mahadavi M et al. Active Immunization with Recombinant PilA protein Protects Against Pseudomonas aeruginosa Infection in a Mouse Burn Wound Model. J Microbiol Biotechnol 2015;25:1538-87.
21. 21. Goudarzi G, Sattari M, Roudkenar MH, Montajabi-Niyat M, Zavaran-Hosseini A, Mosavi-Hosseini K. Cloning, expression, purification, and characterization of recombinant flagellin isolated from Pseudomonas aeruginosa. Biotechnol Lett 2009;31:1353-60.
22. 22. Behrouz B, Amirmozafari N, Khoramabadi N, Bahroudi M, Legaee P, Mahdavi M. Cloning, Expression, and Purification of Pseudomonas aeruginosa Flagellin, and Characterization of the Elicited Anti-Flagellin Antibody. Iran Red Crescent Med J 2016;18:e28271.
23. 23. Babavalian H, Latifi AM, Shokrgozar MA, Bonakdar S, Tebyanian H, Shakeri F. Cloning and expression of recombinant human platelet-derived growth factor-BB in Pichia Pink. Cell Mol Biol (Noisy-le-grand) 2016;62:45-51.
24. 24. Carmichael J, DeGraff WG, Gazdar AF, Minna JD, Mitchell JB. Evaluation of a tetrazolium-based semiautomated colorimetric assay: assessment of chemosensitivity testing. Cancer Res 1987;47:936-42.
25. 25. Hayon T, Dvilansky A, Shpilberg O, Nathan I. Appraisal of the MTT-based assay as a useful tool for predicting drug chemosensitivity in leukemia. Leuk Lymphoma 2003;44:1957-62.
26. 26. Seifi Kafshgari H, Yazdanian M, Ranjbar R et al. The effect of Citrullus colocynthis extracts on Streptococcus mutans, Candida albicans, normal gingival fibroblast and breast cancer cells. J Biol Res 2019;92:30-3.
27. 27. Zorofchian Moghadamtousi S, Karimian H, Rouhollahi E, Paydar M, Fadaeinasab M, Abdul Kadir H. Annona muricata leaves induce G(1) cell cycle arrest and apoptosis through mitochondria-mediated pathway in human HCT-116 and HT-29 colon cancer cells. J Ethnopharmacol 2014;156:277-89.
28. Du GJ, Zhang Z, Wen XD et al. Epigallocatechin Gallate (EGCG) is the most effective cancer chemopreventive polyphenol in green tea. Nutrients 2012;4:1679-91.
29. Kumar S, Sharma VK, Yadav S, Dey S. Antiproliferative and apoptotic effects of black turtle bean extracts on human breast cancer cell line through extrinsic and intrinsic pathway. Chem Cent J 2017;11:56.
30. Fan F, Wey JS, McCarty MF et al. Expression and function of vascular endothelial growth factor receptor-1 on human colorectal cancer cells. Oncogene 2005;24:2647-53.
31. Tebyanian H, Mirhosseiny SH, Kheirkhah B, Hassanshahian M. Isolation and Identification of Mycoplasma synoviae From Suspected Ostriches by Polymerase Chain Reaction, in Kerman Province, Iran. Jundishapur J Microbiol 2014;7:e19262.
32. Noorbala A, Mohammad K, Bagheri YSA, Yasemi MT. Study of mental health status in people 15 years of age and older in the Islamic Republic of Iran in 1999. Hakim Res J 1381;5:10-1.
33. Aghababa H, Mohabati Mobarez A, Khoramabadi N et al. A comparative approach to strategies for cloning, expression, and purification of Mycobacterium tuberculosis mycolyl transferase 85B and evaluation of immune responses in BALB/c mice. Mol Biotechnol 2014;56:487-97.
34. Aghababa H, Mobarez AM, Behmanesh M, Khoramabadi N, Mobarhan M. Production and Purification of Mycolyl Transferase B of Mycobacterium tuberculosis. Tanaffos 2011;10:23-30.
35. Rai Y, Pathak R, Kumari N et al. Mitochondrial biogenesis and metabolic hyperactivation limits the application of MTT assay in the estimation of radiation induced growth inhibition. Sci Rep 2018;8:1531.
36. Moghadamtousi SZ, Kadir HA, Paydar M, Rouhollahi E, Karimian H. Annona muricata leaves induced apoptosis in A549 cells through mitochondrial-mediated pathway and involvement of NF-kappaB. BMC Complement Altern Med 2014;14:299.
37. Fadok VA, Voelker DR, Campbell PA, Cohen JJ, Bratton DL, Henson PM. Exposure of phosphatidylserine on the surface of apoptotic lymphocytes triggers specific recognition and removal by macrophages. J Immunol 1992;148:2207-16.
38. Elmore S. Apoptosis: a review of programmed cell death. Toxicol Pathol 2007;35:495-516.
39. Mohammad RM, Muqbil I, Lowe L et al. Broad targeting of resistance to apoptosis in cancer. Semin Cancer Biol 2015;35 (Suppl):S78-S103.
40. Ouyang L, Shi Z, Zhao S et al. Programmed cell death pathways in cancer: a review of apoptosis, autophagy and programmed necrosis. Cell Prolif 2012;45:487-98.
41. Pereira FV, Melo AC, de Melo FM et al. TLR4-mediated immunomodulatory properties of the bacterial metalloprotease arazyme in preclinical tumor models. Oncoimmunology 2016;5:e1178420.
42. Findley HW, Gu L, Yeager AM, Zhou M. Expression and regulation of Bcl-2, Bcl-xl, and Bax correlate with p53

status and sensitivity to apoptosis in childhood acute lymphoblastic leukemia. Blood 1997;89:2986-93.

43. Tang N, Ma L, Lin XY et al. Expression of PHF20 protein contributes to good prognosis of NSCLC and is associated with Bax expression. Int J Clin Exp Pathol 2015;8:12198-206.
44. Fan H, Li X, Wang W et al. Effects of NMDA-Receptor Antagonist on the Expressions of Bcl-2 and Bax in the Subventricular Zone of Neonatal Rats with Hypoxia-Ischemia Brain Damage. Cell Biochem Biophys 2015;73:323-30.
45. Lee JY, Jee SB, Park WY et al. Tumor suppressor protein p53 promotes 2-methoxyestradiol-induced activation of Bak and Bax, leading to mitochondria-dependent apoptosis in human colon cancer HCT116 cells. J Microbiol Biotechnol 2014;24:1654-63.
46. Zhou FF, Yan M, Guo GF et al. Knockdown of eIF4E suppresses cell growth and migration, enhances chemosensitivity and correlates with increase in Bax/Bcl-2 ratio in triple-negative breast cancer cells. Med Oncol 2011;28:1302-7.
47. Stark AM, Hugo HH, Tscheslog H, Mehdorn HM. p53, BCL-2 and BAX in non-small cell lung cancer brain metastases: a comparison of real-time RT-PCR, ELISA and immunohistochemical techniques. Neurol Res 2007;29:435-40.
48. Youle RJ, Strasser A. The BCL-2 protein family: opposing activities that mediate cell death. Nat Rev Mol Cell Biol 2008;9:47-59.
49. Finucane DM, Bossy-Wetzel E, Waterhouse NJ, Cotter TG, Green DR. Bax-induced caspase activation and apoptosis via cytochrome c release from mitochondria is inhibitable by Bcl-xL. J Biol Chem 1999;274:2225-33.
50. Bashyam MD. Understanding cancer metastasis: an urgent need for using differential gene expression analysis. Cancer 2002;94:1821-9.
51. Leake I. Colorectal cancer. Understanding the routes of metastasis in colorectal cancer. Nat Rev Gastroenterol Hepatol 2014;11:270.
52. Sun SY. Understanding the Role of the Death Receptor 5/FADD/caspase-8 Death Signaling in Cancer Metastasis. Mol Cell Pharmacol 2011;3:31-4.
53. D'Arrigo G, Navarro G, Di Meo C, Matricardi P, Torchilin V. Gellan gum nanohydrogel containing anti-inflammatory and anti-cancer drugs: a multi-drug delivery system for a combination therapy in cancer treatment. Eur J Pharm Biopharm 2014;87:208-16.
54. Lu J, Zhang K, Nam S, Anderson RA, Jove R, Wen W. Novel angiogenesis inhibitory activity in cinnamon extract blocks VEGFR2 kinase and downstream signaling. Carcinogenesis 2010;31:481-8.
55. Goel HL, Mercurio AM. VEGF targets the tumour cell. Nat Rev Cancer 2013;13:871-82.
56. Ferrara N. VEGF and the quest for tumour angiogenesis factors. Nat Rev Cancer 2002;2:795-803.
57. Shibuya M. Vascular Endothelial Growth Factor (VEGF) and Its Receptor (VEGFR) Signaling in Angiogenesis: A Crucial Target for Anti- and Pro-Angiogenic Therapies. Genes Cancer 2011;2:1097-105.